Electronic Supplementary Material (ESI) for Journal of Materials Chemistry A.

Supporting Information

3Mg/Mg_2Sn Anodes with Unprecedented Electrochemical Performance towards Viable Magnesium-ion Batteries

Amol Bhairuba Ikhe, Su Cheol Han, S. J. Richard Prabakar, Woon Bae Park,* Kee-Sun Sohn,* and Myoungho Pyo*

A. B. Ikhe, Dr. S. C. Han, Dr. S. J. R. Prabakar, Prof. W. B. Park, Prof. M. Pyo
Department of Printed Electronics Engineering, Sunchon National University, Chonnam 57922, Republic of Korea
E-mail: wbpark@scnu.ac.kr, mho@sunchon.ac.kr
Prof. K.-S. Sohn
Faculty of Nanotechnology and Advanced Materials Engineering, Sejong University, Seoul 05006, Republic of Korea
E-mail: kssohn@sejong.ac.kr

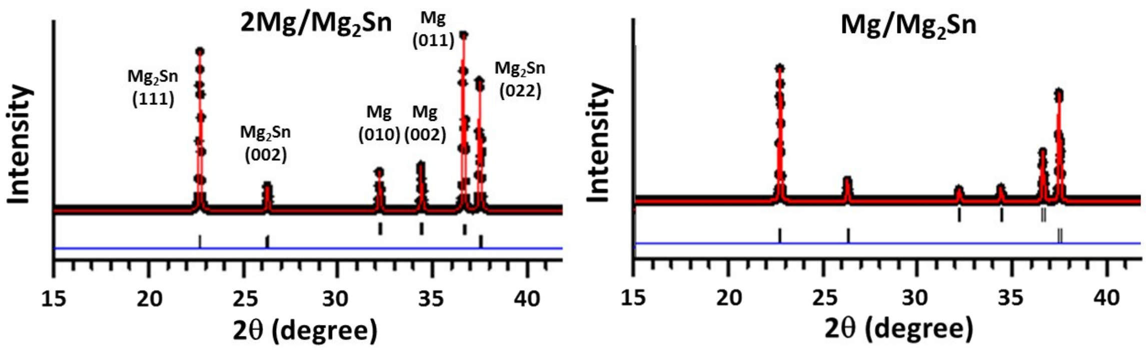

Fig. S1. Simulated XRD pattern for nMg/Mg_2Sn. Vertical tick marks above the blue line represent the Bragg's reflections for Mg and Mg_2Sn phases. For obtaining a simulated pattern, the Fullprof program was set to Pattern calculation (X-ray). The structural parameters were obtained from ICSD collection codes 53767 and 151368 for Mg and Mg_2Sn phases, respectively. Arbitrary values for the scale factor of the two phases were chosen in such a way that the phase fractions obtained after the simulation meet the desired ratio, i.e. Mg:Mg_2Sn = 1:1 and 1:2. Peak shape and peak width was modeled using a Pseudo-Voigt function and a Caglioti equation for FWHM, respectively.

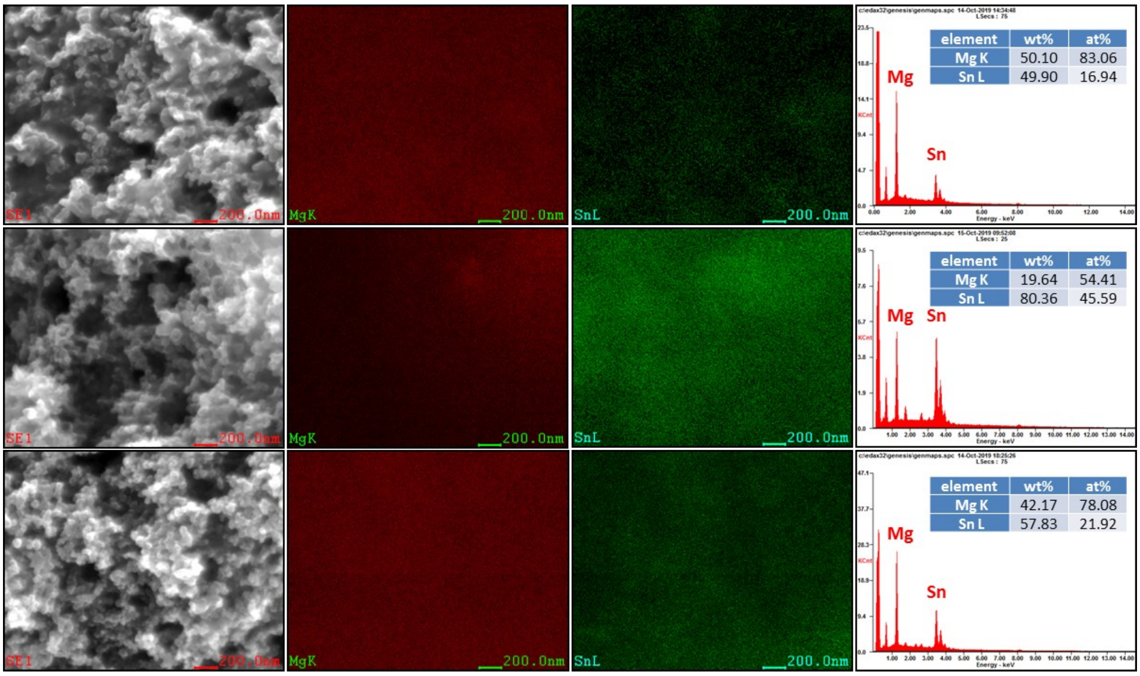

Fig. S2. FESEM images, elemental maps, and EDX spectra for (top) pristine, (middle) 1st demagnesiated, and (bottom) re-magnesiated $3Mg/Mg_2Sn$.

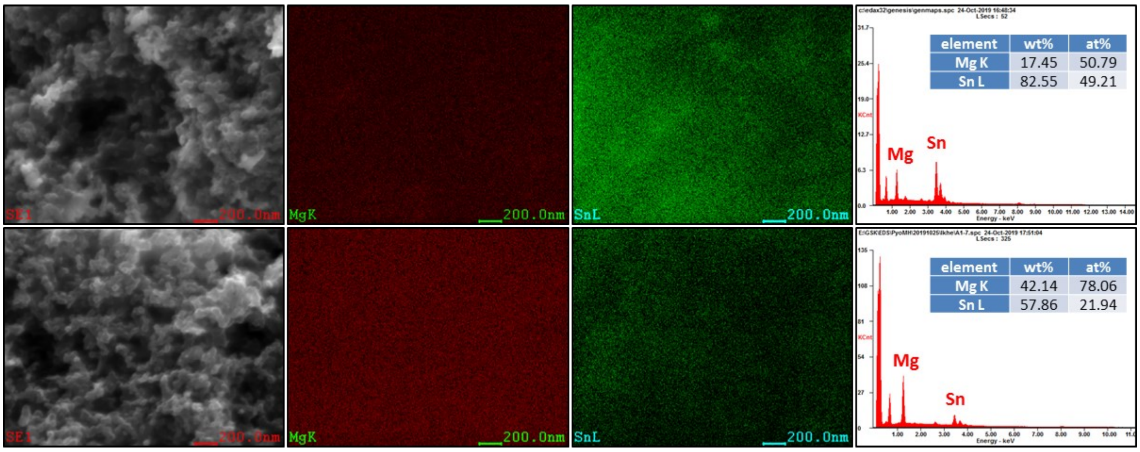

Fig. S3. FESEM images, elemental maps, and EDX spectra for (top) demagnesiated, and (bottom) magnesiated $3Mg/Mg_2Sn$ after 3 C/D.

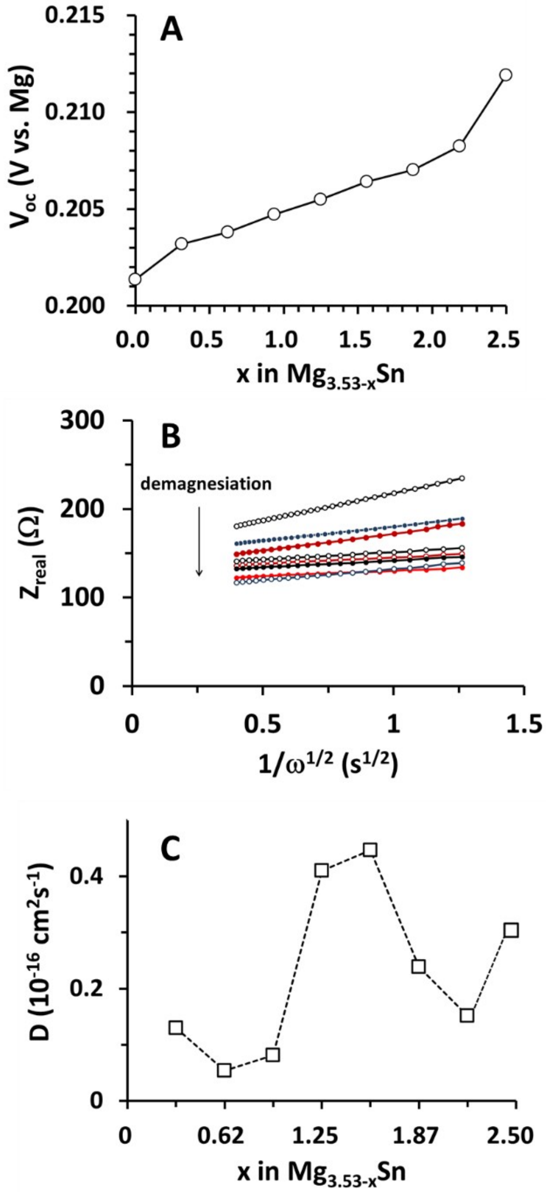

Fig. S4. (A) Coulometric titration curve determined using a galvanostatic intermittent titration technique. (B) Warburg plot obtained from Fig. 5C. (D) Evolution of diffusion coefficients (Ds) at different stages of magnesiation. The Ds were calculated using a Warburg constant (σ) that was determined from a slope in (B) and the equation $\sigma = V_M \cdot (dV_{oc}/dx)/(zFAm(2D)^{0.5})$, in which V_M is the molar volume of Mg_2Sn (46.6 cm^3 mol^{-1}), z is the charge of mobile ions (2), F is the Faraday constant (96485 C mol^{-1}), A is the BET surface area (65.2 m^2 g^{-1}; We used the BET value determined for de-magnesiated 3Mg/Mg_2Sn.), and m is the mass of active materials.

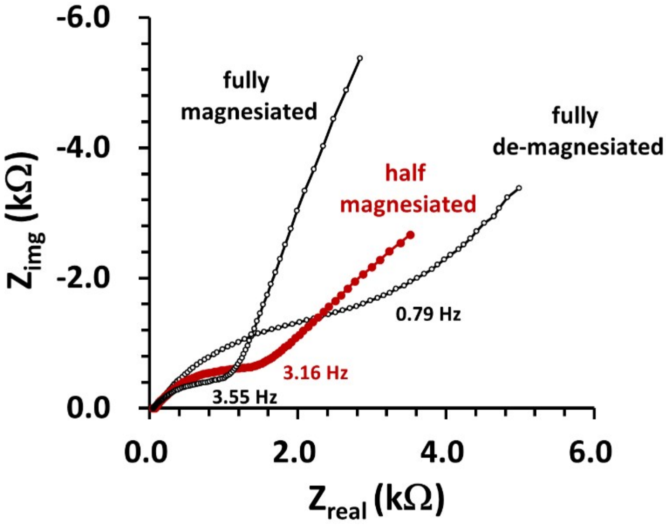

Fig. S5. EIS spectra of Mg_2Sn after 3 C/D cycles. Frequencies were changed within 0.1 and 100 kHz. In contrast to the behaviors of $3Mg/Mg_2Sn$, impedances were increased with de-magnesiation.

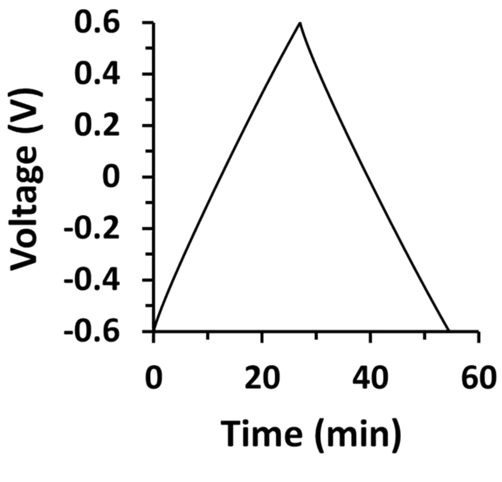

Fig. S6. Galvanostatic C/D curves of an AC symmetric cell at 10 mA g^{-1} in $Mg(TFSI)_2$/acetonitrile. The capacitance of the AC was calculated to be 56.7 F g^{-1}.

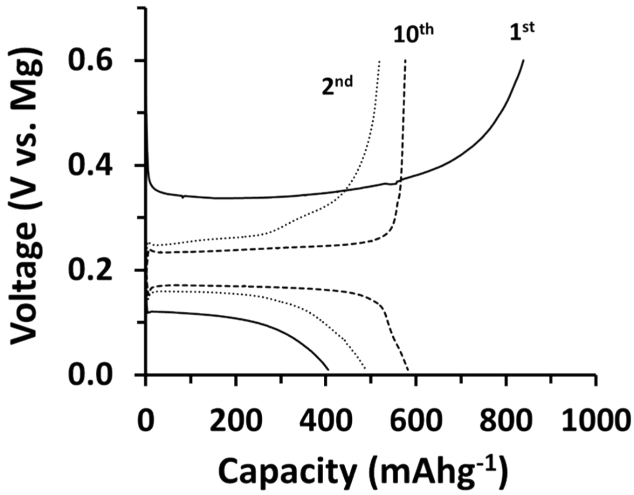

Fig. S7. C/D profiles of pristine $3Mg/Mg_2Sn$ in $Mg(TFSI)_2$:$MgCl_2$(0.5M:0.5M)/diglyme at 200 mA g^{-1} with Mg metal as a reference electrode. No low-voltage process appeared during the 1st de-magnesiation, with a low discharge capacity. Though the reversibility was evident, the subsequent C/D cycles delivered inferior capacities. Stable plateau voltage behaviors were reached after 10 C/D cycles, by contrast to those of $3Mg/Mg_2Sn$ in $Mg(HMDS)_2$:$MgCl_2$/THF.

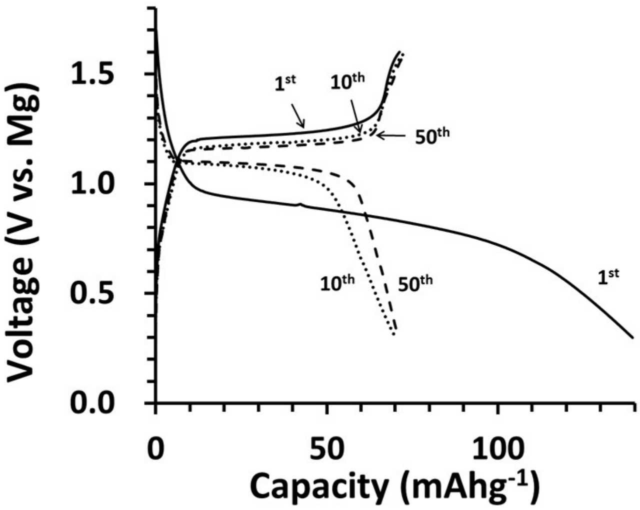

Fig. S8. C/D profiles of Mo_6S_8 in $Mg(HMDS)_2$:$MgCl_2$/THF using Mg metal as a reference electrode. Profile shapes and capacities were similar to those obtained in $3Mg/Mg_2Sn$|$Mg(HMDS)_2$:$MgCl_2$/THF|Mo_6S_8 (Fig. 6C). Current density = 12.8 mA g^{-1}.